Current generation with low-frequency waves

Nathaniel J. Fisch and Charles F. F. Karney

Plasma Physics Laboratory, Princeton University, Princeton, New Jersey 08544
(Received 17 December 1979; accepted 9 October 1980)

Various types of traveling waves may be injected into a tokamak to continuously sustain the toroidal current. Interest in this problem arises from the possibility of operating tokamak reactors in the steady state. The low-frequency waves most suitable for this task are identified in terms of the power cost for deployment in a reactor. Means of exciting these waves and tradeoffs with design criteria are discussed. A comparison is made with the alternative attractive regime of high-frequency waves. Conclusions are based, in part, on the numerical solution of the two-dimensional Fokker–Planck equation with an added quasi-linear term due to the waves.

I. INTRODUCTION

One of the drawbacks of the tokamak approach to fusion power is that it is, in its simplest form, based on a pulsed device, limited by the volt-seconds attainable in the Ohmic transformer coils. This difficulty can be circumvented, in theory, by generating the toroidal plasma current with radio-frequency (rf) waves, which may be injected continuously. The waves would have a net toroidal component of momentum, so that, when absorbed by the electrons, a force is exerted that drives a toroidal electric current. For practical employment in a reactor, the power required to drive the current may only be a small fraction of the fusion power output. Not all types of waves incur the same power dissipation. Thus, in searching for the most favorable waves to drive current, we must consider not only the ease with which the wave can be excited, but also their individual power requirements.

There are two wave regimes that are attractive in terms of minimizing the power dissipated for a given current generated, namely, low and high parallel phase velocity waves. The former regime of subthermal phase velocities was suggested by Wort[1] and is attractive because in this regime waves have a high momentum content per unit energy. In other words, whereas the momentum in a wave is proportional to its wavenumber, k, the energy carried by the wave is proportional to its frequency, ω, so that waves with low ω/k_z have a high parallel momentum content (where k_z is the wavenumber in the toroidal direction). When the energy of such waves is absorbed by electrons, the momentum absorbed is proportionately higher. Wort envisioned the use of subthermal-parallel-phase-velocity, low-frequency compressional Alfvén waves to achieve current generation. In this context, we consider the low-frequency regime to be synonymous with the low-phase-velocity regime.

The alternative approach of using waves with high-phase velocities was pointed out by Fisch.[2] Although waves here have little momentum content, their momentum and energy are absorbed by fast electrons. The electrons that carry the current are relatively collisionless and so retain their momentum longer than the thermal electrons which carry the current when low-phase-velocity waves are employed. The relative infrequency of collisions encountered by the current carriers compensates for the dearth of momentum in the driving waves. This approach was originally envisioned employing the lower-hybrid wave with a phase velocity parallel to the magnetic field several times the electron thermal velocity.

Numerical studies[3] of the use of high-phase-velocity waves, improving on the accuracy of the original analytical studies, have pinpointed the amount of power dissipated for given generated current. Before a systematic comparison can be made of the two phase velocity regimes with the goal of recommending one regime over the other for application to tokamak reactors, an accurate calculation must also be made of the power dissipated by the low-phase-velocity waves. The task that we set forth for ourselves in this paper is to identify the relevant parameters in low-phase-velocity current drive and to numerically determine the power requirements in this operating regime, thereby enabling comparison with the alternative regime.

The task of evaluating the low-phase-velocity mechanism of current drive is broader than that of the high-phase-velocity mechanism and the numerical computations are trickier. The parameter space to be explored is larger since, as we shall see, it includes the wave type and wave amplitude. The paper is organized as follows: In Sec. II, we derive the acceleration of electrons due to waves of various types. In particular, we consider transit-time magnetic pumping, Landau damping, and the combination of the two that results when Alfvén waves are employed.

The steady-state power dissipated and the steady-state current generated result from a balance between the absorption of wave energy and momentum by resonant electrons and the collisional processes which distribute the absorbed energy and momentum to all particles of both species. In Sec. III, we show how these effects may be described by the linearized Fokker–Planck equation, but with the drift of the electron population in parallel velocity space self-consistently included, a detail that could be safely ignored only in the high-phase-velocity regime. In Sec. IV, we describe our numerical approach to solving the Fokker-Planck equation, comparing various numerical techniques.

In Sec. V, we sort through the large parameter space of dependencies to isolate those relevant to reactor applications. We numerically determine the resistance

 0031-9171/81/010027-13$00.90

encountered by the rf-driven currents for each type of acceleration mechanism and as a function of wave amplitude and spectrum location. The most important wave regime is that of low-phase velocity and low amplitude. Exemplary cases in this wave regime are described in greater detail in Sec. VI.

In Sec. VII, we consider the question of wave excitation. Having numerically determined the plasma resistance to current-drive by various waves, we explore trade-offs between minimizing the power dissipation and relaxing other design features. The comparison of the two wave regimes in terms of suitability for application to reactors is developed in Sec. VIII. In that section, we write the fraction of the fusion power output used to drive the waves as a function of macroscopic parameters only, such as temperature, density and reactor dimensions. In Sec. IX, we present our conclusions, including a perspective on related effects not considered in this study.

II. THE WAVE DIFFUSION COEFFICIENT

The force exerted on electrons in a large, steady magnetic field B_0 in the direction parallel to the field may be written as

$$m\frac{dv_z}{dt} = -eE_z - \mu\frac{\partial B_z}{\partial z}, \tag{1}$$

where $\mu \equiv mv_\perp^2/2B_0$ is the magnetic moment and the z direction is taken to be parallel to the steady magnetic field. In our application to the torus, we will employ the approximation that these field lines point in the toroidal direction, ignoring any actual discrepancy between the toroidal and parallel directions. Equation (1) is valid in the small electron gyroradius limit, i.e., $k_x\rho_e \ll 1$ (where k_x is the perpendicular wavenumber), which is always the case in our applications. The field components E_z and B_z represent traveling waves in the z direction and will be related in a manner dependent on the plasma dispersion. For example, it is possible to excite electrostatic waves so that only E is nonzero in Eq. (1). These waves are Landau damped by electrons resonant with the wave. In the event that the waves are uncorrelated, there results diffusion of the electrons in parallel velocity space, i.e., in the absence of other effects we may write

$$\frac{\partial f}{\partial t} = \frac{\partial}{\partial v_z} D_{rf}(v_z)\frac{\partial}{\partial v_z} f, \tag{2}$$

where f is the electron distribution function. Here, the quasi-linear diffusion coefficient is due to Landau damping, i.e., $D_{rf} = D_L$, which is given by

$$D_L(v_z) = \frac{16\pi^2 e^2 \mathcal{E}_{kz}}{m^2 v_z}\bigg|_{k_z=\omega/v_z}. \tag{3}$$

If the spectral energy density $\mathcal{E}_{kz}$ is centered at k_0 corresponding to phase velocity v_{z0} and spread over a narrow width Δ_k of parallel wavenumbers, we can approximate

$$D_L(v_z) = \begin{cases} \dfrac{\pi e^2\langle E_z^2\rangle}{m^2 v_{z0}\Delta_k}, & v_{z1} < v_z < v_{z2} \\ 0, & \text{otherwise}, \end{cases} \tag{4}$$

where $\langle\ \rangle$ denotes time average, and we identified v_{z1} and v_{z2}, respectively, as the slowest and fastest parallel phase velocities in the spectrum. We note that describing the wave-particle interaction as a diffusion phenomenon is strictly valid only when the wave spectrum is sufficiently broad. However, in the case at hand, where we intend to balance the wave-particle effects against collisional effects, which are turbulent, it would, in fact, be appropriate to use the diffusion equation even when the wave is fully coherent. This is true even if the trapping time for the wave is shorter than the collision time, because we are interested in the behavior of the distribution function f over times longer than a collision time. The effect of the trapping is approximately to flatten the distribution function over a trapping width after several collision times, which is the same effect exhibited by Eq. (2).

It is possible that E_z in Eq. (1) vanishes, so that only the traveling magnetic field accelerates the electrons. This mechanism is called "transit-time magnetic pumping." By strict analogy with the Landau damping case, merely substituting the magnetic acceleration term for the electric acceleration term, we can form a diffusion equation of the form of Eq. (2), except that the diffusion coefficient is

$$D_m(v_z) = \begin{cases} \dfrac{\pi e^2\mu^2 k_z^2\langle B_z^2\rangle}{m^2\Delta_k v_{z0}}, & v_{z1} < v_z < v_{z2} \\ 0, & \text{otherwise}. \end{cases} \tag{5}$$

The main difference between D_L, as defined in Eq. (4), and D_m is that D_m exhibits a strong dependence on $v_\perp$, namely, $D_m \sim v_\perp^4$. We will find that this preferential diffusion of high-$v_\perp$ electrons, which are relatively collisionless, plays an important role in reducing the effective plasma resistivity to currents generated by magnetic pumping.

The transit-time magnetic pumping is, however, the sole diffusion mechanism only when the plasma conductance can be ignored. For most applications, the plasma will itself generate an E_z field, so that both right-hand side terms in Eq. (1) are present.[4,5] The origin of the E field, as argued by Stix,[5] is the low-frequency magnetic field fluctuations which set up parallel ion density fluctuations. Quasi-neutrality is achieved by means of a self-consistent electric field E_z which acts on hot electrons. This reasoning follows only from the assumption that $\mathbf{E} + \mathbf{v}_f \times \mathbf{B} = 0$, where $\mathbf{v}_f$ is the fluid velocity, and this assumption certainly is valid in plasmas of interest. The resulting E_z field can be related to the fluctuating B_z field by

$$E_z = -\left(\frac{v_{te}^2}{\Omega_e}\right)\left(\frac{\partial B_z}{\partial z}\right), \tag{6}$$

where Ω_e is the electron gyrofrequency. Using Eq. (6) in Eq. (1), we can write the force equation for electrons as

$$m\frac{dv_z}{dt} = \frac{e}{2\Omega_e}(2v_{te}^2 - v_\perp^2)\frac{\partial B_z}{\partial z}. \tag{7}$$

Note that the Landau damping and magnetic pumping forces are always out of phase, the former force domi-

nating for $v_\perp$ small and the latter for $v_\perp$ large. This is in contrast to the force equation for the ions, wherein these two forces would be in phase and additive. For the electrons there is, in fact, an exact cancellation of these forces when $v_\perp^2 = 2v_{te}^2$.

By analogy with the Landau damping and magnetic pumping cases, we can write the diffusion coefficient for low-frequency waves in a conductive plasma as

$$D_A(v_z) = \begin{cases} \frac{\pi}{4}\frac{e^2k_z^2}{\Delta_k v_{z0}}\frac{\langle B_z^2\rangle}{B_0^2}(2v_{te}^2 - v_\perp^2)^2, & v_{z1} < v_z < v_{z2} \\ 0, & \text{otherwise.} \end{cases} \tag{8}$$

Our later interest will be focused on diffusion due to Alfvén waves, a particular case of the low-frequency waves just treated. Hence, we will refer to D_A as the Alfvén wave diffusion coefficient. Our concern will center on whether the Alfvén wave diffusion is more similar to diffusion by Landau damping or magnetic pumping, given that it retains canceling terms due to both mechanisms. Of special interest and to be determined numerically is whether the currents generated by the Alfvén wave encounter the reduced resistivity that is expected in the case of magnetic pumping.

Throughout this paper we assume that the diffusion coefficient for any of the three mechanisms is finite only in a cylindrical or disk-shaped region of velocity space, i.e., $v_{z1} < v_z < v_{z2}$, with no other dependence on v_z, but with a $v_\perp$-dependence characteristic of the wave type. Although for a broad spectrum of waves this modeling is reasonable, in the event of single-wave excitation the shape of the resonant region can be quite different. For example, in the case of magnetic pumping, the resonant region would be shaped in the form of the complement of a cone, since the trapping width of the single wave varies as $(\mu k_z B_z)^{1/2}$. What we wish to show now is that this distinction in the shape of the resonant region is immaterial for parameters of interest in reactors. Hence, considering the resonant region as disk shaped is sufficiently general. The relevant regime for reactors, as we shall see later, is in the limit of low D_0 and for a narrow spectrum of wave parallel phase velocities.

To demonstrate the equivalence of the two representations of the shape of the resonant region, consider the power dissipated as a function of $v_\perp$, which we may write as

$$P_d(v_\perp) = \int \frac{n_0 m v^2}{2}\frac{\partial f}{\partial t}\,dv_z = -\int_{v_{z1}}^{v_{z2}} n_0 m v_z D_{rf}\frac{\partial f}{\partial v_z}\,dv_z$$

$$\approx -n_0 m D_{rf} f(v_\perp, v_{z0})\Delta_v v_{z0}^2/v_{te}^2, \tag{9}$$

where Δ_v is the width of the resonant region, i.e., $\Delta_v = v_{z2} - v_{z1}$, and D_{rf} is assumed small enough so that $f(v_z)$ remains essentially Maxwellian. In addition, we have assumed that Δ_v is small compared with v_{z1}, except possibly at large $v_\perp$ where this assumption need not hold since negligibly few electrons would be affected. The point is that, in this limit, $P_d(v_\perp)$ depends only on the product $D_{rf}\Delta_v$ rather than on D_{rf} and Δ_v individually. The task is to show that the perpendicular dependence of this product is the same whether one employs the many-wave limit, disk-shaped region, or the single-wave limit, complement-of-a-cone shaped region. Should the perpendicular dependence of P_d be identical, we can assume that the other dynamics in the problem are also identical.

Note that in the many-wave limit $D_{rf} \sim A^2$, where A denotes the relevant acceleration term in Eq. (1). For example, for magnetic pumping, we would have $D_{rf} \sim (v_\perp^2 B_z)^2$. In the opposite limit, trapping occurs and we have instead $\Delta_v \sim A^{1/2}$, where Δ_v now exhibits a $v_\perp$ dependence. Since the limit of resonance broadening is now applicable, we also have[6] $\Delta_v \sim D_{rf}^{1/3}$. Thus, in either limit $\Delta_v D_{rf} \sim A^2$, so that the dependence of P_d on $v_\perp$ is identical, and the resulting dynamics is indistinguishable. We choose to concentrate our numerical work on the many-wave case because the variation in D_{rf} is more easily handled than the variation in Δ_v, due to the finite grid spacing. We bear in mind, however, that our results, in this limit, can also be applied to the trapping limit.

III. MODELING THE COLLISIONS

According to the quasi-linear diffusion equation (2), the waves deposit energy into the distribution of electrons until f is a constant where D_{rf} is finite so that the effect saturates. In practice, collisions prevent the plateau in f from forming and allow a realistic steady-state distribution function to be obtained wherein energy is continuously deposited by the waves into the resonant particles and collisions redistribute this energy amongst all the particles.

In order to model the behavior of the distribution function under these circumstances, we add a Fokker-Planck collision term $(\partial f/\partial t)_c$ to Eq. (2), i.e., we write

$$\frac{\partial f}{\partial t} = \frac{\partial}{\partial v_z} D_{rf}\frac{\partial}{\partial v_z} f + \left(\frac{\partial f}{\partial t}\right)_c. \tag{10}$$

For many purposes, it is convenient to rewrite Eq. (10) as

$$\frac{\partial f}{\partial t} = -\nabla_{\mathbf{v}}\cdot\mathbf{S} = -\nabla_{\mathbf{v}}\cdot(\mathbf{S}_{rf} + \mathbf{S}_e + \mathbf{S}_i), \tag{11}$$

where $\mathbf{S}_{rf} = -D_{rf}\,\partial f/\partial v_z\,\hat{z}$ and $\mathbf{S}_e$ and $\mathbf{S}_i$ are the fluxes of electrons due to collisions off the electron and ion backgrounds, respectively.

The current J produced by the wave and the power P_d dissipated by the wave are given by

$$J = -en_0\int v_z f\,d\mathbf{v}, \tag{12}$$

$$P_d = -mn_0\int v_z D_{rf}\frac{\partial f}{\partial v_z}\,d\mathbf{v} = \int \mathbf{v}\cdot\mathbf{S}_{rf}\,d\mathbf{v}. \tag{13}$$

The task facing us is to solve Eq. (10) for the various forms of wave diffusion D_{rf}, to determine J and P_d in the steady state, and finally to assess the feasibility of current drive by waves.

Since we are primarily interested in the steady-state solutions to Eq. (10), the question arises as to the cir-

cumstances under which Eq. (10) has a useful steady-state solution. In a realistic situation (e.g., in a reactor), the steady state is maintained by a balance of several sources and sinks of energy, momentum, etc. In writing Eq. (10), we have already considerably simplified this picture by ignoring the spatial variations of f, and the presence of sources (e.g., alpha particle heating) and sinks (e.g., radiation). This is done because by ignoring the additional terms we are able to concentrate on the physics of the rf current-drive and we do not have to make numerous *ad hoc* assumptions as to the way these terms enter. Unfortunately, Eq. (10) as it stands does not approach a steady state since there is no way for the energy deposited by the waves to be lost. We correct this deficiency by calculating $(\partial f/\partial t)_c$ assuming that the background electrons and ions are Maxwellians of equal and constant temperatures T. We may picture the flow of energy as follows: Energy is deposited into the electrons by the waves; this is transferred, via collisions, into the bulk electrons, conceptually treated as a separate background species (a small fraction of energy also goes to the bulk ions); the energy is then lost to the system in some unspecified way. Although we employ equal background electron and ion temperatures in our numerical studies, it should be appreciated that our conclusions are sensitive only to the background electron temperature.

The assumption of Maxwellian backgrounds solves the problem of energy equilibration. The other important physical quantity we must consider is the parallel momentum. Radio-frequency current-drive deposits momentum in a selected class of particles. The rate at which this momentum is lost determines the efficiency of the process. Although the mechanism for momentum loss in tokamaks is not well understood, it is likely that momentum in the electrons is first lost to the ions before being lost by the plasma (e.g., by collisions with neutrals). We therefore take the ion background to be stationary, but allow the electron background species to drift. The amount of the drift is determined by requiring that the total force F on the electron test species due to the electron background species is zero, so that the momentum is lost by the electrons only via the ions. We may write this condition as

$$F \equiv m n_0 \int S_{ez}\, d\mathbf{v} = 0 . \tag{14}$$

It should be understood that Eq. (14) is to be solved implicitly for the electron drift velocity.

We should emphasize that although we have been forced to adopt an approximate model of collisions, our approach yields no less accurate results than approaches which do treat collisions exactly and are computationally more time consuming. Consider, for example, the alternative approach which would disdain linearizing the Fokker–Planck equation and would attempt an exact treatment of the collision terms. This was the approach originally envisioned by Rosenbluth *et al.*,[7] who suggested an efficient expansion of the collision operator in Legendre harmonics. Treating the collision operator exactly, however, immediately implies that other assumptions must be introduced to assure that a steady state is reached. (Not reaching the steady state would itself introduce other uncertainties.) Thus, in the absence of accurate models for sources and sinks of particles, momentum, and energy, an absence that, in fact, may be safely assumed, the "exact" treatment of the collision operator would not yield more precise answers to the questions that we ask here.

To summarize the treatment of the collision term: $(\partial f/\partial t)_c$ is calculated assuming constant temperature Maxwellian background electrons and ions (see, for instance, Trubnikov[8]). The ions are taken to be stationary while the electrons drift parallel to the magnetic field with velocity v_d which is chosen to satisfy Eq. (14). As in Ref. 3, we chose $T_i/T_e = 1$ and $m_i/m_e = 1836$. The solution is insensitive to the precise magnitude of these two quantities. We would, for instance, have obtained the same results had we taken a much larger mass ratio. In addition, since we are concerned with applications to fusion reactors, we take the ion charge state Z_i to be 1.

Having taken the background temperatures to be constant, it is then convenient to normalize velocities to the electron thermal velocity and times to the collision time. Thus, we define $\mathbf{u} = \mathbf{v}/v_{te}$, $w = v_z/v_{te}$, $s = v_\perp/v_{te}$, and $\Delta = \Delta_v/v_{te}$, where $v_{te} = (T/m_e)^{1/2}$. Similarly, we introduce $\tau = \nu_0 t$ where

$$\nu_0 = \frac{\log\Lambda\,\omega_{pe}^4}{2\pi n_0 v_{te}^3} , \tag{15}$$

where $\log\Lambda$ denotes the Coulomb logarithm. The azimuthal angle θ is defined by $\theta = \cos^{-1}(w/u)$. The wave diffusion coefficient is normalized to $\nu_0 v_{te}^2$:

$$D(w,s) = \frac{D_{rr}}{\nu_0 v_{te}^2} = \begin{cases} D_L = D_0(w) , \\ D_m = D_0(w) s^4 , \\ D_A = D_0(w)(2-s^2)^2 , \end{cases} \tag{16}$$

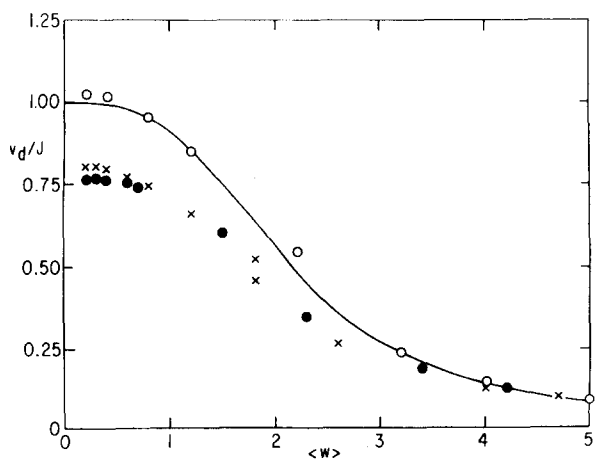

FIG. 1. v_d/J vs $\langle w\rangle \equiv (w_1 + w_2)/2$ for the cases of Landau damping (open circles), magnetic pumping (×'s), and Alfvén waves (closed circles) in the low-D_0 limit. Here, we took $D_0 = 0.001$. The solid curve is given by $J/P_d = (1 + 0.1\langle w\rangle^3)^{-1}$ and is a rough semianalytic fit to the data. No attempt was made to optimize this fit. Cylindrical coordinates were employed for $\langle w\rangle \leq 1.8$ and spherical coordinates were employed for $\langle w\rangle \geq 1.8$.

where we have explicitly written out the velocity space dependencies of D for the cases of Landau damping, magnetic pumping, and Alfvén wave excitation, respectively. We shall take $D_0(w)$ to be equal to D_0 (a constant) for $w_1 < w < w_2$ and to be zero elsewhere.

Other physical quantities are made dimensionless by multiplying them by the relevant powers of v_{te}, ν_0, the electron charge density $-en_0$, and the electron mass density mn_0. In particular, J is normalized to $-en_0v_{te}$ and P_d to $m_e n_0 \nu_0 v_{te}^2$.

The importance of including the drift can be seen from Fig. 1, where we compare the drift with the current produced by the damping of waves of various phase velocities. When the normalized phase velocity w is large, v_d scales as J/w^3, a result anticipated by Ref. 2. Thus, the results of Ref. 3, which dealt with the large w limit but neglected the drift, are not materially modified by the drift. For w small, the case treated in this paper, the drift is roughly equal to J. Thus, we expect the drift to make a significant difference to the ratio J/P_d. This is what is observed numerically: This ratio calculated including the drift is about twice its value without the drift.

IV. NUMERICAL SOLUTION OF THE FOKKER-PLANCK EQUATION

The program used to solve Eq. (10) is essentially the same as that used in Ref. 3. Three modifications were made to that program: Firstly, following the suggestion of Ref. 9, we changed the way in which the collisional friction terms in Eq. (10) are computed. This makes the steady-state solution obtained numerically with no rf very close to a Maxwellian.

Secondly, we added the capability of solving Eq. (10) in cylindrical coordinates (w, s) as well as in spherical coordinates (u, θ). The spherical version treats the collision term fully implicitly while the cylindrical version treats the rf diffusion term fully implicitly. Which version is used depends on how important are the terms which are treated explicitly. Generally, all the work with waves at high-phase velocities was performed in spherical coordinates. Cylindrical coordinates were used for the cases where the rf phase velocity was small, although the spherical version could also be used if the wave amplitude was small.

The third change made was to allow the background electrons to drift. As discussed in the previous section, this drift was chosen to make the force of the background electrons on the test electrons equal to zero. The force F was computed using the appropriate discrete representation of the integral in Eq. (14). (This was determined by demanding that the parallel momentum be conserved in the discrete system.) It was only necessary to recompute the drift once every 20 steps. The additional computation was then small compared with the rest of the program.

The majority of the numerical results presented here were obtained using the cylindrical version of the program. The domain of integration, when using cylindrical coordinates, was $|w| \leq 3$ and $s \leq 5$. The grid size was 0.1 in both directions and the time step was 0.01. The initial conditions were taken to be a Maxwellian

$$f(\tau = 0) = f_M(u) \equiv (2\pi)^{-3/2} \exp(-\tfrac{1}{2}u^2) . \tag{17}$$

Generally, integration of Eq. (10) to $\tau = 30$ was sufficient to obtain a steady state.

The chief difficulty in interpreting the results arises because of the finite grid size. This means there is some uncertainty as to the location of the spectrum in velocity space which introduces a systematic error into the results obtained by the cyclindrical version. In order to gauge the magnitude of this effect, we ran several of the cases, for which D and w were small, with the spherical version and with various grid sizes. The discrepancy between the results obtained by the two versions of the program was about 10%.

V. NUMERICAL CALCULATION OF RESISTANCE

The resistance of the plasma to rf-driven currents depends on the type of wave, the wave phase velocity, and the wave amplitude. To see how these dependencies arise, we first analytically consider the linear regime, $D \to 0$, which will enable us to develop an intuition about the problem, to establish notation, and to determine the relevant scalings. The numerical findings will then be presented in light of the qualitative analytic arguments.

In the linear regime, the power dissipated can be computed from the direct damping of the waves on an unperturbed Maxwellian electron distribution. Using Eq. (9), but now writing all quantities in normalized units, we find

$$\begin{aligned} P_d &\equiv \int_0^\infty 2\pi s\, ds \int_{-\infty}^{\infty} P_d(w,s)dw \equiv \int_0^\infty 2\pi s P_d(s)\, ds \\ &= 2\pi f(w_1, 0) \int_0^\infty s e^{-s^2/2} \int_{-\infty}^{\infty} w^2 D(w,s) dw\, ds , \end{aligned} \tag{18}$$

where we assumed that $\Delta w_1 \ll 1$ so that f may be taken as independent of w over the resonant region. For later convenience, we related the quantities P_d, $P_d(s)$, and $P_d(w,s)$, which are distinguished by their arguments and represent the density of power dissipation in configuration space plus the argument space. Assuming that $D(w,s)$ is as given by Eq. (16), i.e., finite only for w between w_1 and w_2, wherein it is only s dependent, we can write

$$P_d = \frac{w_2^3 - w_1^3}{3} f(w_1, 0) \int_0^\infty D(w_1, s) e^{-s^2/2}\, 2\pi s\, ds . \tag{19}$$

The calculation of the current in the linear regime is more difficult, since it necessarily involves calculating distortions from the Maxwellian distribution. However, we can derive a scaling law. First note that the incremental energy W absorbed by an electron moving with parallel velocity w is related to the incremental momentum P absorbed by

$$W = wP . \tag{20}$$

The power dissipated in the steady state can be obtained

by differentiating Eq. (20) to obtain

$$P_d(w,s)=\frac{\partial W}{\partial t}=w\frac{\partial P}{\partial t}\equiv w\nu(w,s)P\,, \tag{21}$$

where $\nu(w,s)$ is the rate at which collisions destroy momentum absorbed at coordinates (w,s). Since the momentum is directly related to the current, we can write, in normalized notation,

$$J(w,s)/P_d(w,s)=[w\nu(w,s)]^{-1}\,. \tag{22}$$

Equation (22) determines the amount of current present in the steady state, i.e., when the collisional destruction of momentum balances the steady absorbtion of momentum at (w,s). Using Eqs. (18) and (22), we find that the total current density is given by

$$J=\int_0^\infty 2\pi s\,ds\int_{-\infty}^{\infty}\nu^{-1}wDf\,dw\,. \tag{23}$$

For $w\ll 1$, ν becomes dependent on s only. Assuming then w_1, $w_2\ll 1$ and $D(w,s)=D(w_1,s)$ between w_1 and w_2 and is zero elsewhere as in Eq. (16), we get

$$J=\frac{w_2^2-w_1^2}{2}\int_0^\infty 2\pi s\,D(w_1,s)\nu^{-1}(w_1,s)e^{-s^2/2}f(w_1,0)\,ds\,. \tag{24}$$

Comparing Eqs. (19) and (24), we find the scaling

$$J/P_d=\frac{3}{2}\left(\frac{w_2^2-w_1^2}{w_2^3-w_1^3}\right)C_W\equiv\frac{C_W}{w_a}\,, \tag{25}$$

where Eq. (25) defines w_a, an average resonant w, and C_W is independent of the spectrum location, depending only on the wave type, i.e., the dependence of D on s in Eq. (16).

We expect that the linear theory given by Eqs. (19), (24), and (25) will be valid when D is small enough. In this limit, both J and P_d are linear functionals of the wave spectrum in that contributions to these quantities arising from several spectra are purely additive. While $\nu(0,s)$ is not known precisely, certain conclusions can still be drawn. To the extent that ν is due to ion pitch-angle scattering, we have $\nu\sim s^{-3}$. Although

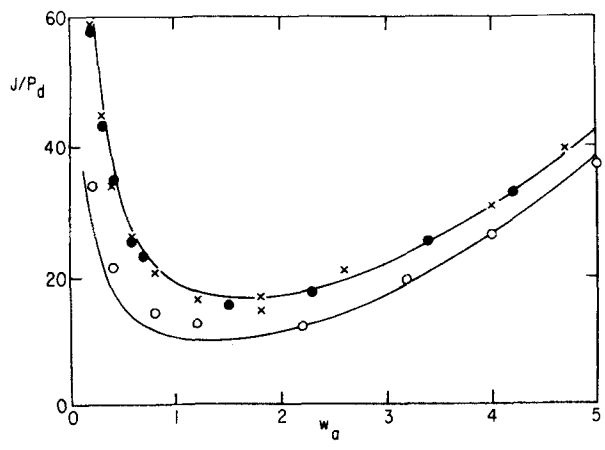

FIG. 2. J/P_d vs w_a for each of the three cases. Symbols have the same meaning as in Fig. 1. The solid lines are rough semianalytic fits to the data. No attempt was made to optimize the fit. The upper line obeys $J/P_d=13/w_a+1.4w_a^2+5$ and the lower line obeys $J/P_d=8/w_a+1.4\omega_a^2+2$. Coordinates were employed as in Fig. 1.

the energy scattering by electrons somewhat alters this picture, we still expect that $\nu^{-1}(0,s)$ is larger for larg-larger s. Thus, comparing Eqs. (19) and (22), we can conclude that waves which induce diffusion at larger s will have a larger J/P_d.

The ratio J/P_d has been numerically determined for a wide range of parameters. In Fig. 2 we display J/P_d as a function of the weighted parallel velocity w_a, defined by Eq. (25). The various wave types are displayed separately; we use x's, closed circles, and open circles to denote, respectively, magnetic pumping, Alfvén waves, and Landau damping. The solid lines are semianalytic fits to the data and will be explained. We took $D_0=10^{-3}$ throughout in order to approach the linear limit (although, obviously, finite D_0 will always appear large somewhere, say, as $s\to\infty$). In all cases tabulated in Fig. 2, we took $\Delta=0.2$. A separate check of isolated cases showed that D_0 was small enough so that a larger Δ would produce a J and P_d that represented only additive contributions of narrower spectra.

The salient feature of Fig. 2 is that, in fact, the analytic scaling given by Eq. (25) is justified in the limit $w_a\to 0$. The constant C_W may be determined numerically to fit the data for each wave. It is found that

$$C_A\approx C_m\approx 13\,, \tag{26a}$$

$$C_L\approx 8\,, \tag{26b}$$

where C_A, C_m, and C_L represent the appropriate C_W to be used in Eq. (25) and, respectively, denote the cases of Alfvén waves, magnetic pumping and Landau damping.

As we pointed out in Sec. IV, there is some uncertainty in the data for the low-w cases due to the poor resolution of the computer grids. The results in Fig. 2 for $w_a<1$ were obtained using the cylindrical version of the program. Since the edges of the rf spectrum line up with the grid in this case, the errors that arise because of the uncertainty of the spectrum location are systematic. We can therefore be confident that the agreement in the $1/w_a$ scaling between the analytical and numerical results is real. Comparisons with the spherical version which predicts a somewhat larger J/P_d, indicate that the constants C_W may be in error by as much as 10%.

In the opposite limit, that of high w_a, the Landau damping, magnetic pumping, and Alfvén wave results become identical. In this limit, J/P_d is proportional to a weighting of w^2 over the resonant interval.[2] For the narrow spectra that we chose to plot in this limit, the exact weighting is immaterial with corrections only of order Δ/w. We numerically find $J/P_d\approx 1.4\,w_a^2$, where the constant 1.4 is found by fitting the data over an admittedly short range in w. This constant roughly agrees with that found in previous numerical studies,[3] which dealt with the high-D limit.

Since the low-w_a approximation vanishes at high w_a, whereas the high-w_a approximation vanishes at low w_a, we can uniformly approximate J/P_d by adding the li-

miting forms. Thus, we write

$$J/P_d = C_W/w_a + 1.4\, w_a^2, \tag{27}$$

where the coefficients C_W are given by Eqs. (26). We should point out that although we do expect all cases to exhibit the same asymptotic behavior $J/P_d \sim w_a^2$, for w_a large, we also expect a wave-dependent first-order correction to this result. This correction would be given by $J/P_d \sim w_a^2 + y_W$ where y_W is a constant dependent on the wave type. In the case of magnetic pumping or Alfvén waves, we expect y_W to be larger than in the Landau damping case, since the current carriers are situated at higher $v_\perp$. Although a good analytic fit to the numerical data could be obtained with Eq. (27), a slightly better fit can be obtained by adding the y_W term. The uniform approximation, including a roughly fit y_W term, is shown as solid lines in Fig. 2 for either case. (The Alfvén wave and magnetic pumping cases are grouped here as one case.) An excellent fit to the data is obviously obtained.

The three curves of Fig. 2 converge at large w_a because, in that limit, the collisionality of the resonant electrons is dominated by their parallel velocity so that the resistance is relatively insensitive to exactly where in $v_\perp$ space the momentum is absorbed. For precisely the same reason there is little dependence on the magnitude of D_0 in this limit. The independence from D_0 does not, however, hold true in the low-velocity regime. For example, while displaying a significant variation at low D_0, J/P_d for the three waves at large D_0 must become identical, since the effect of each of the waves is the same, to completely flatten the resonant region is parallel velocity space. In Fig. 3 we show the dependence on D_0 for the three waves for excitation between $w_1 = 0.1$ and $w_2 = 0.3$. As expected from the argument given here J/P_d for the three waves does converge for D_0 large. Furthermore, note that for each wave J/P_d monotonically decreases with D_0. This results because, with increasing D_0, the wave damping at high $v_\perp$ becomes saturated sooner than at low $v_\perp$, where the resonant electrons are far more collisional. The current is then generated, to an increasing extent by the low-$v_\perp$ collisional electrons,

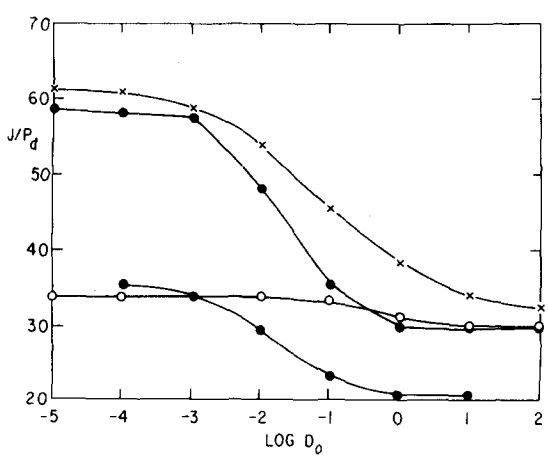

FIG. 3. J/P_d vs $\log_{10} D_0$. Symbols have the same meaning as in Fig. 1. The three upper curves, converging at large D_0, are for $w_1 = 0.1$ and $w_2 = 0.3$. The lowest curve is for Alfvén waves with $w_1 = 0.3$ and $w_2 = 0.5$.

thus encountering greater resistance.

The increase in resistance with higher D_0 saturates when the resonant region is plateaued also for small $v_\perp$. At the other extreme, the decrease in resistance with lower D_0 saturates when electrons are not plateaued anywhere except at very high $v_\perp$, where there are exponentially few electrons. The crossover between these two limits is most dramatic for the Alfvén wave and magnetic pumping cases, where J/P_d changes by over a factor of 2. It is not difficult to analytically estimate the crossover point. Assume that most of the power is dissipated in the linear regime at $s = s_0$. Then, as D_0 increases, we expect the most dramatic change in J/P_d to occur when the power dissipation saturates, i.e., when the distribution function is flattened in w space at $s = s_0$. This occurs when the collisional diffusion equals the wave diffusion, i.e., when

$$D \approx s_0^{-3} \equiv D_{x\sim 0}(D/D_0), \tag{28}$$

where $D_{x\sim 0}$ should be the coefficient D_0 at the crossover point to the large-D_0 limit. From Eq. (19), the distribution of $sP_d(s)$ for large s is given, in the linear limit, by

$$sP_d(s) \propto s^5 e^{-s^2/2}, \tag{29}$$

since for large s and for magnetic pumping and Alfvén waves, $D \sim s^4$. The factor of s is included to reflect that due to the cylindrical geometry, the dissipation region is larger at larger s. From Eq. (29), we easily determine that the most power is dissipated at $s_0 = \sqrt{5}$. Using Eq. (28), we determine $D_{x\sim 0} \approx 4 \times 10^{-3}$, which should be independent of w for w small. Although this derivation is admittedly crude, the result is consistent with Fig. 2 not only for the spectrum spanning 0.1–0.3, but also for the spectrum spanning 0.3–0.5, which displays the same crossover characteristics.

It is interesting to compare the numerical results with Wort's original calculation. He approximated J/P_d based on an argument that does not distinguish wave type, amplitude, or phase-velocity regime. He reasoned that all the absorbed momentum would be distributed equally among all electrons, resulting in a drifting Maxwellian electron distribution. The resulting current is then assumed to obey Spitzer resistivity. Since the redistribution of momentum conserves momentum but not energy, the overall power dissipation is increased by the ratio of w_a to v_d, the electron drift velocity. Thus, Wort predicted that the total power dissipated would be $P_d = \eta_{Sp} J^2 w_a / v_d$, where η_{Sp} is the Spitzer resistivity. Actually, Wort's reasoning should lead to about twice this power dissipated, since a drifting Maxwellian population encounters, roughly, twice the Spitzer resistivity. It turns out, however, that (in normalized form) Wort's result is $J/P_d \approx 15\, w_a^{-1}$, which can be seen from Eq. (27) to be in fairly good agreement with the numerical results for Alfvén waves or magnetic pumping in the limit of low D and low w_a.

VI. THE STEADY-STATE DISTRIBUTION

Since the cases of greatest interest are those for which the spectrum width is narrow and D is small, we

undertake a closer examination of typical cases in this regime. The steady-state distribution function f in this regime is close to a Maxwellian, so in order to see what is happening in the steady state, we look at δf, the difference between f and f_M and at the flux S.

Figure 4 shows $\delta f = f - f_M$ for $w_1 = 0.1$ and $w_2 = 0.3$ for each of the three wave types. D_0 is chosen to be 10^{-4} so we are well into the linear regime, as can be seen from Fig. 2. The finite value of D at $s = 0$ for Alfvén wave excitation and Landau damping causes a density depression for $u < w_1$. This is isotropized by the strong pitch angle scattering by the ions. For magnetic pumping, D vanishes at $s = 0$, and the depression is absent. However, in all three cases, the drift of the background electrons causes a sympathetic drift in the test electrons. This is visible as a density increase at $w \sim 1$ and a corresponding decrease at $w \sim -1$. The effect of the null in the Alfvén wave diffusion coefficient at $s = \sqrt{2}$ can be clearly seen.

In the steady state, the flow is incompressible, i.e., $\nabla_u \cdot \mathbf{S} = 0$. Therefore, rather than plotting the flux as a two-dimensional vector field it is more convenient to plot the streamlines of the flow. The flux S is tangential to these streamlines. Plots of the streamlines for the three cases shown in Fig. 4 are shown in Fig. 5. These show a much greater variety than the plots of δf. The two extremes are given by the cases of magnetic pumping and Landau damping. In the case of Landau damping, the competition between the tendency of the wave to flatten the distribution in the parallel direction and that of ion collisions to flatten it in the azimuthal direction causes a strong flux in the s direction in the resonant region. This flux closes on either side of the spectrum. This picture is very similar to that seen with high-phase-velocity waves.[3] In the case of magnetic pumping, we again have a component of flux in the s direction in the resonant region, but this is superimposed on a stronger flux in the plus or minus w direction. This is caused by the quartic dependence of D on s, which drives electrons at high s (where the diffusion is strong) in the plus w direction. The particles are able, however, to cross the resonant region against the

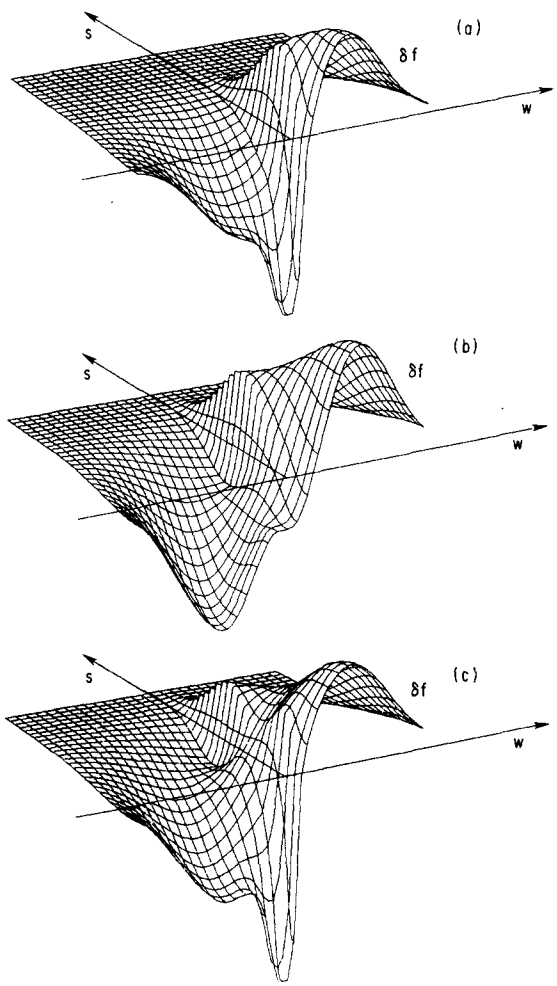

FIG. 4. Plots of $\delta f(w, s)$ for the cases of (a) Landau damping, (b) magnetic pumping, and (c) Alfvén wave excitation. In each case, $D_0 = 10^{-4}$, $w_1 = 0.1$, and $w_2 = 0.3$. The data are plotted for $-3 \leq w \leq 3$ and $0 \leq s \leq 5$.

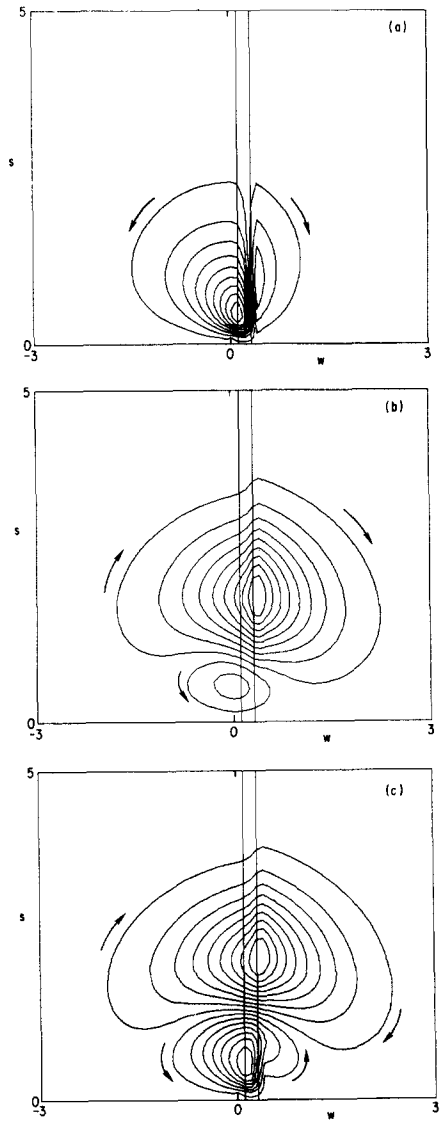

FIG. 5. The streamlines of the flux S for the three cases (a), (b), and (c) given in Fig. 4. The arrows indicate the direction of the flux. Equal amounts of flux flow between adjacent contours. The vertical lines represent the limits of the resonant region.

direction of collisionless diffusion at lower s where D is much smaller. The smaller eddy seen at $s<1$ is not directly caused by the wave but arises because of the relative drift of the ion and electron backgrounds. The streamlines for the Alfvén wave damping are a composite of the two previous cases.

We now wish to depict by means of two transitional cases, a change in the topology of the streamlines as the wave spectrum is driven at higher phase velocities. Figure 6 shows the streamlines for the case of magnetic pumping for two larger phase velocities. As w_1 and w_2 are increased, the flux in the resonant region becomes more nearly parallel to the s direction and this flux can close on either side of the spectrum. Both these features are seen in the streamlines for the Landau damping case, Fig. 5(b). Indeed, as the phase velocity of the waves is increased, the patterns of the streamlines for all three types of waves approach those of the high-D Landau damping case (cf. Ref. 3). However, in the case of magnetic pumping, this is accomplished through the emergence of an x point in the flux field [located at $w\approx 0$, $s\approx 2$ in Fig. 6(b)]. Similarly, although we do not show it, an x point develops in the flux field in the case of high-phase-velocity Alfvén waves.

VII. EXCITING THE ALFVÉN WAVE

In order to evaluate the attractiveness of driving steady-state currents in a tokamak reactor with low-frequency waves, we must first determine the most efficient excitation structure for the waves. We envision that the generated current is substantial enough so that the reactor can be continuously operated, and that the most efficient means of excitation incurs the least power dissipation. We bear in mind, however, that the optimum wave parameters may involve concessions in other aspects of the reactor design.

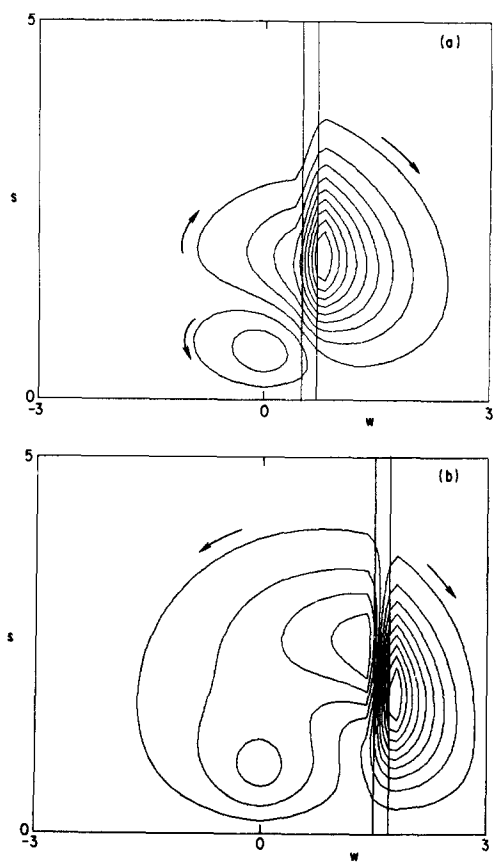

FIG. 6. The streamlines of the flux S for magnetic pumping with $D_0=10^{-4}$ and (a) $w_1=0.5$, $w_2=0.7$, (b) $w_1=1.5$, $w_2=1.7$.

Firstly, as we showed in Sec. V, the type of wave is of crucial importance. Far less power dissipation is incurred in the use of transit-time magnetic pumping as an acceleration mechanism than in the use of electrostatic parallel electric fields (Landau damping). As pointed out in Sec. II, when $\mathbf{E}+\mathbf{v}_f\times\mathbf{B}\approx 0$, there will always result a parallel electric field accompanying the magnetic pumping. This results in the Alfvén-wave type of the acceleration mechanism that is, in fact, comparable to magnetic pumping in terms of efficiency. In the following, we assume excitation only of waves with this characteristic.

For maximum efficiency in generating current, the Alfvén wave should possess the richest momentum content yet avoid depositing its energy to the ions. The damping on the ions will be nearly absent if v_z is large enough, say, several times the ion thermal velocity. This locates v_z at roughly six times the ion thermal velocity since the momentum content of the wave is highest at low v_z, while the ion damping sets in abruptly when v_z enters the range of the thermal ions. It is convenient to define

$$\alpha\equiv\omega/k_z v_{ti}\,, \tag{30}$$

and the argument given here implies that $\alpha\approx 6$ yields the maximum efficiency for current drive.

Although choosing α large enough avoids ion Landau damping at the fundamental harmonic, the ions remain susceptible to damping at higher harmonics of the ion cyclotron frequency. In order to avoid this damping at higher harmonics, ω should be chosen to be less than half the ion cyclotron frequency. This assures that all resonant phase velocities, $(\omega\pm n\Omega_i)/k_z$, with n an integer, fall at least as far outside the bulk ion distribution as does ω/k_z. Thus, if the fundamental harmonic incurs only negligible ion damping, so will the higher harmonics.

Finally, we prefer, of course, that the power dissipation be subject to the "low-D" limit as depicted in Fig. 3. It turns out that this regime is indeed attainable for reactor parameters. We defer, however, the justification of this point until the next section, wherein reactor-relevant calculations are presented. Here, we turn instead to the question of how these high-efficiency waves, presumably also in the favorable low-D regime, can, in fact, be excited.

In the stipulated frequency range $\omega\ll\Omega_i$, compressional Alfvén waves can be excited. These waves have the dispersion relation $\omega=kv_A$, where v_A is the Alfvén speed. Due to the inhomogeneity of the plasma these waves couple to the shear Alfvén waves at the shear Alfvén resonance, $\omega=k_z v_A$. At the resonance the wave is mode-converted to a kinetic-Alfvén wave[10] which is

strongly damped on the electrons. The energy thus dissipated will also generate current. The rate γ at which energy in the compressional Alfvén wave is damped in this wave is given by[11]

$$\gamma/\omega \approx (\omega/\Omega_i)(k_z x')^{2/3}, \tag{31}$$

where x' is the inhomogeneity scale length at the shear Alfvén resonance. We have assumed that the wave has no poloidal variation and that the lowest-order radial mode is excited. The dominant factor here is ω/Ω_i, which expressed in terms of α becomes

$$\omega/\Omega_i = \alpha n(\rho_i/R), \tag{32}$$

where n is the toroidal mode number, R is the tokamak major radius and ρ_i is the ion Larmor radius. Taking $\alpha \sim 6$, $n \lesssim 10$, and $\rho_i/R \lesssim 10^{-3}$, we see that ω/Ω_i and hence γ/ω are very small. We shall see from Eq. (39) that the normal damping for the compressional Alfvén waves is roughly $w\omega$ where w is the normalized phase velocity of the wave. Since $w \sim 10^{-1}$, this damping is usually much larger than that due to the shear Alfvén resonance. We therefore neglect the coupling to the shear Alfvén resonance in what follows.

The compressional Alfvén wave dispersion relation can be written as

$$k_x^2 + k_z^2 = \omega^2/v_A^2, \tag{33}$$

where k_x is the wavenumber perpendicular to the magnetic field but parallel to the density and temperature gradients. Variation in the poloidal direction is not helpful and we assume there is none. Using Eq. (30) in Eq. (33), yields the convenient form

$$k_x^2 = k_z^2(\alpha^2\beta/4 - 1), \tag{34}$$

where β is the average toroidal beta, neglecting alpha particle pressure, defined by

$$\beta \equiv \frac{n_0(T_i + T_e)}{B_T^2/2\mu_0} \approx \frac{4n_0 T \mu_0}{B_T^2}, \tag{35}$$

where B_T is the toroidal magnetic field. We assume that β is given in any particular reactor design and that Eq. (34) represents a constraint on our choice of k_x and k_z in choosing the most favorable α, i.e., $\alpha \approx 6$.

In fact, except for very high-β operation, the most favorable α cannot be obtained with the most efficient coupling, i.e., when k_x and k_z are real and represent resonant cavity modes with

$$k_z = n/r, \tag{36a}$$

$$k_x \approx l\pi/a, \tag{36b}$$

where n and l are integers. [Equation (36b) is only an approximate relation as discussed, e.g., in Ref. 5.] As can be seen from Eq. (33), the wave parallel phase velocity travels faster than the Alfvén speed for k_x real. Unless the Alfvén speed is very slow (β large), α cannot be as small as desired.

The alternative is to impose the desired parallel phase velocity, allowing, if need be, k_x to become imaginary. The drawback of this approach is that the wave is inefficiently excited; there is higher reactive power and the losses in the exciting coils are higher. Nevertheless, if the power dissipated in the coils is much smaller than that dissipated in the plasma, this alternative approach could be preferred.

The power dissipated in the coils (per unit plasma volume) may be written as

$$P_c = 2R_s H_z^2(a)/a, \tag{37}$$

where H is the magnetic intensity, a is the minor radius, and R_s is the surface resistivity of the exciting structure which we will assume to be room-temperature copper. The total power dissipated in the coils is thus $(2\pi R)(\pi a^2)P_c$. For reactive modes (k_x imaginary), the traveling magnetic field at the coil surface (which we assume to be at $r = a$) is related to the traveling magnetic field in the plasma center by

$$H_z(a) \approx I_0(\kappa_x a)H_z(0), \tag{38}$$

where $\kappa_x = \mathrm{Im}(k_x)$ and I_0 is the zeroth order modified Bessel function. Since I_0 depends exponentially on $\kappa_x a$, we expect, in view of Eq. (37), that the coil losses will set in abruptly at a few $\kappa_x a$. What we wish to determine now is this "threshold" beyond which coil losses become dominant.

We define this threshold as the magnitude of $\kappa_x a$ for which the power dissipated in the coils equals the power dissipated by the plasma electrons. Assuming that the dissipation in the plasma is linear, i.e., that operation is in the low-D regime, the power dissipated in the plasma is given by

$$P_d \approx (\sqrt{2\pi} w \omega_{pe}^2/\omega_{ce}^2)\omega\mu_0 H_z^2(0), \tag{39}$$

where we assume that the traveling parallel magnetic field in the plasma is given approximately by H_z ($r = 0$). Using Eqs. (37), (38), and (39), we find

$$\frac{P_c}{P_d} = \frac{1}{w}\left(\frac{R_s}{a\omega\mu_0}\right)\left(\frac{2}{\pi}\right)^{1/2}\frac{\omega_{ce}^2}{\omega_{pe}^2} I_0^2(\kappa_x a)$$

$$\approx 4 \times 10^{-7}\frac{\lambda_z^{1/2}}{aw^{3/2}}\frac{T_{10}^{3/2}}{\beta} I_0^2(\kappa_x a), \tag{40}$$

where the second approximate equality assumes room-temperature closely spaced copper coils, and λ_z and a are given in meters and T_{10} is the plasma temperature normalized to 10 keV. The threshold wavenumber is obtained when

$$\kappa_x a \approx \pi, \tag{41}$$

which corresponds to $P_c/P_d \approx 1$ when $T_{10} \approx 1$, $\beta \approx 5\%$, $w \approx 0.1$, and $\lambda_z \approx a \approx 1$. The threshold is, however, insensitive to the precise plasma and wave parameters. Thus, Eq. (41) may be taken as a restriction on κ_x in any reactor environment.

These alternatives and restrictions are graphically displayed in Fig. 7. Lines of constant α for a given β emanate from the origin at varying slopes. If a waveguide mode is to be excited (k_x real), then operation is favored at $k_x \approx \pi/a$ and $k_z = n/R$, where n is an integer and is taken as large as possible. The minimum α in this scheme is $\alpha = 2/\beta^{1/2}$, which is optimum for $\beta \approx 10\%$ but not for smaller β. The main tradeoff here is smaller α versus a large number of coils to define a high-n mode. There is also a theoretical limitation on n due

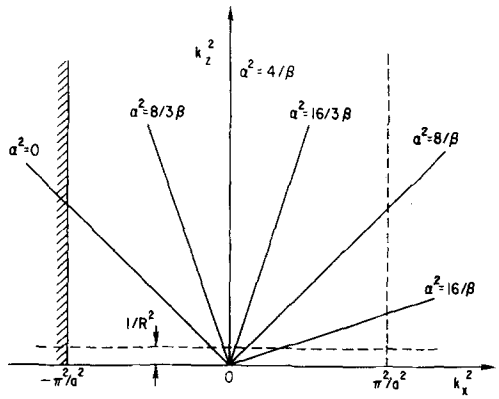

FIG. 7. Grid of mode numbers. The hatched region is forbidden due to large coil losses. For a given β, $\alpha<6$ is forbidden due to ion Landau damping. For clarity, the line $1/R^2$, corresponding to $n=1$, is drawn higher than for most R/a.

to the condition $\omega<\Omega_i/2$, but this limit, $n<\Omega_i R/(12v_{ti})$, is not approached in practice.

The alternative favors low-k_z operation, the minimum allowable k_z being $k_z=1/R$. Here, k_x is allowed to be imaginary in order to lie on the line of most favorable α, which for $\beta<10\%$ will be located in the upper-left quadrant. For κ_x to be minimized, representing less damping in the coils, it is desirable to have low k_z. If k_z is not very small, and should β be so low that this corresponds to $\kappa_x^2>\pi^2/a^2$, operation in this regime is not worthwhile.

Assuming no dissipation other than in the plasma or the coils, Fig. 7 indicates, for the usual reactor parameters, that an $n=1$ traveling Alfvén wave, with k_x imaginary, is the best course to follow in order to minimize the power dissipated. However, in practice, the plasma-coil system is itself contained in the reactor walls, which may be conducting, and hence subject to eddy-current losses. We make no attempt here to look for an optimization to this larger problem. However, we should note that in the event that the first conducting wall is at least a minor radius away from the Alfvén-wave coils, the reactive magnetic field is not so compressed that the losses in the wall exceed those in the coils. An optimized design of the first wall would introduce sufficient insulating breaks to minimize the field compression and prevent the wall currents from producing a cancelling magnetic field in the plasma. It should be emphasized that the alternative option wherein plasma waveguide modes are excited, does not require tampering with the first wall. The optimized design would examine the trade-off between the decreased dissipation in the plasma in the reactive limit at the expense of redesigning or relocating the first wall.

VIII. APPLICATION TO A REACTOR

The primary application of driving currents with low-frequency waves is the continuous operation of a tokamak reactor through the indefinite sustaining of the poloidal magnetic field. In this context, the amount of power required to maintain the current is of crucial importance. Minimizing this power dissipation relies on the excitation of the most favorable waves, as discussed in Sec. VII, which includes the attainment of the low-D regime. We point out in this section that the low-D regime is, in fact, attainable, and we compare low-frequency waves to high-frequency waves as mechanisms of current generation.

Supplying the current necessary to achieve continuous operation implies that the poloidal magnetic field B_p is completely sustained by the wave-generated current J. By Ampère's law we have

$$B_p=\mu_0 aJ/2\,. \tag{42}$$

We assume that operation is achievable at $\beta_p=R/a$, where we define

$$\beta_p\equiv\frac{n_0(T_e+T_i)}{B_p^2/2\mu_0}\approx\frac{4n_0T\mu_0}{B_p^2}\,, \tag{43}$$

where we assumed, for convenience only, $T_e\approx T_i$. Combining Eqs. (42) and (43) and making use of the assumed operating regime for B_p, we can write

$$J=4\left(\frac{n_0T_e}{\mu_0 aR}\right)^{1/2}=1.4\times10^6\left(\frac{n_{14}T_{10}}{a_1R_1}\right)^{1/2}\frac{\mathrm{MA}}{\mathrm{m}^2}\,, \tag{44}$$

where a_1 and R_1 are, respectively, the minor and major radii given in meters, where n_{14} is the density normalized to 10^{14} cm^{-3} and where T_{10} is the temperature normalized to 10 keV. The normalized J, that we make more frequent use of than the dimensional J, can now be written as

$$J=4\frac{c}{\omega_{pe}\sqrt{aR}}\approx2.1\times10^{-4}(n_{14}a_1R_1)^{-1/2}\,, \tag{45}$$

where c is the velocity of light. For $a_1R_1\approx25$, $n_{14}\approx1$, and the spectrum situated at, say $0.1<w<0.3$, the required normalized D to drive the normalized current given by Eq. (45) is about 7×10^{-5}, which is well into the low-D regime, as can be seen from Fig. 3.

Having ascertained that operation in the low-D regime is attainable in typical reactors near the optimum spectrum location (i.e., low w), we can make use of Eqs. (26) and (27) to write the crucial parameter

$$\epsilon\equiv\frac{P_d}{P_f}\approx\frac{0.95\log\Lambda}{(n_{14}T_{10}a_1R_1)^{1/2}}\frac{P_d/J}{(3T_{10}-2)}\,, \tag{46}$$

where P_f is the fusion power density and P_d is the rf-power dissipated in the plasma. On the right-hand side of Eq. (46), all quantities are normalized; P_d/J is as given by Eq. (27). In writing the right-hand side of Eq. (46), we linearized the dependence of P_f on temperature, so that P_f agrees with the exact fusion power density at $T_{10}=1$ and $T_{10}=2$. This linearization supplies a good fit for the regime of first-generation D-T reactors, which will employ a plasma temperature roughly between 10 and 20 keV.

Equation (46) is valid in the high-phase-velocity limit as well as for low-phase-velocity waves. In the limit of fast waves, Eq. (46) reduces to previously obtained results. (The numerical factor given in Ref. 2 is incorrect, however, the detailed studies reactor, performed by Ehst,[12] do employ a correct version of this equation.) In order to compare the two main wave re-

gimes wherein current generation appears attractive, we look for the most favorable parameters that we can expect in each regime. For high-phase-velocity waves, such as lower-hybrid waves, we can expect $w_a \approx 4-4.5$. For low-phase-velocity waves, we can expect $w_a \approx 0.1-0.2$. Obviously, it would be preferable to have even faster waves in the former regime and even slower waves in the latter regime. However, in hot plasmas the wave accessibility represents a severe limit on the fastest phase velocity, which at $w_a \approx 4$ is nearly the speed of light. The restrictions on the low-frequency waves have been discussed in Sec. VII. Using the expected optimal parameters for each regime, we see from Eq. (46) that to generate the same current in reactors, the low-frequency regime operation requires in the range of 30%–50% as much power as the high-frequency regime.

The attractiveness of the low-frequency regime relative to the high-frequency regime is more dramatic when we consider operation in high-β reactors and nearer to the range of 20 keV than 10 keV. Because of accessibility requirements, the high frequency spectrum must be placed at relatively slow w_a, mitigating the advantage of these waves. This constraint does not apply to the low-frequency spectrum, which interacts even at the higher temperatures mainly with nonrelativistic resonant electrons. Thus, in high-temperature, high-β reactors, the low-frequency method becomes even more attractive.

Before concluding this section, two important points need to be made. Firstly, the estimates of power dissipation represent an ideal situation, wherein all power is dissipated in the electrons and the efficiency of generating the wave power and delivering it to the reactor has not been included. Yet, factors of two are quite important here. For typical reactor parameters, current generation with lower-hybrid waves could ideally be in the range of $\epsilon \approx 5\%$.[2,3,12] When the nonideal effects are included, we can expect a true circulating power on the order of 15%. This is a substantial yet feasible circulating power. However, it is also in the range where a factor of three reduction, such as might be obtained with Alfvén waves, could be of crucial importance to the overall economic attractiveness of steady-state operation.

The last point to be made here is that the overriding concern may be for the type of launching scheme for the waves. Waveguides are very convenient structures for bringing lower-hybrid waves into the plasma. The use of coils, for exciting low-frequency waves, is problematic in reactor plasmas. The attractiveness of the Alfvén waves will depend on whether suitable shielding can be provided for the launching structure. What we have shown here is that should the shielding problem be solved, the power requirements for low-frequency rf-current drive compare favorably with the high-frequency method.

IX. CONCLUSIONS

The thrust of this paper has been to determine the parameters relevant to driving currents with low-frequency waves. We found that sufficient current for steady-state reactor operation could be obtained with low-amplitude waves (low-D limit), which are to be preferred, and we numerically calculated the power cost for such operation. This result is summarized by Eq. (46), which displays, as a function of design parameters, the fraction of fusion power output that must be recycled to support the steady-state current.

The comparison with the alternative method, current generation with lower-hybrid waves, is facilitated by Eq. (46). The conclusion is that the power requirements for Alfvén-wave current generation can be significantly less, especially in high-β, high-temperature reactors. In the 10 keV temperature range and assuming $\beta \geq 5\%$, Alfvén waves can drive currents with less than half the power required for lower-hybrid waves. In the 20 keV temperature range, the accessibility condition on lower-hybrid waves becomes more severe with the consequence that Alfvén waves are relatively more attractive. Certainly in later-generation advanced-fuels reactors, the temperature would be so high that the fast wave regime would not be competitive in terms of power cost.

In our calculations we have not included a number of effects that could possibly affect the power dissipation. We indicate here our expectation that these effects can be safely neglected. For example, consider the collisional dissipation in the nonresonant particles that support the wave. Although this dissipation can be important in changing the power requirements in the high-frequency method of current drive, it cannot be important in the low-frequency case. This is because it is mainly the nonresonant electrons, being lighter than the ions, that absorb this power and with it they also absorb the wave momentum. Since the collisionality of nonresonant electrons does not differ significantly from that of the resonant electrons in the case of low-frequency current drive, the wave momentum absorbed in such a manner will result in an additional current with much the same characteristics. In particular, we have in mind that J/P_d would not be significantly different. This reasoning does not pertain to the high-frequency case, where the nonresonant electrons are far more collisional than the resonant electrons, so that care must be taken that the resonant region does not become so flattened in parallel velocity space that the nonresonant absorbtion dominates.[2]

We have also ignored radiation losses from the plasma. In the case of low-frequency waves, the electron distribution function remains nearly Maxwellian, so that radiation losses should not be any greater than when the current is driven by the conventional Ohmic transformer coils. In fact, the losses could be smaller because no runaway electrons are produced. This reasoning would not apply to the case of high-frequency waves, which produce a large distortion from the Maxwellian distribution at high velocities. In such a case, radiation losses become more important, although not necessarily intolerable.

These two effects, collisional absorption and radiation losses, pertained more to the case of high-frequency

than low-frequency current drive. Now, we turn to an effect that has far more relevance to the low-frequency case, namely, the neoclassical effects of trapped electrons. In the case of lower-hybrid waves, the resonant electrons are nearly all circulating. The current carried by slower electrons is negligible in any case, so that trapped-nonresonant-electron effects can hardly matter. On the other hand, in the low-frequency case, nearly all the electrons that absorb the wave energy and momentum are trapped and hence they carry no current.[13] This would appear to render our calculations inapplicable except near the magnetic axis where there are no trapped electrons.

Nonetheless, for steady-state reactor operation, the fact that the resonant electrons are trapped presents no problem. Here we sketch the argument, also given elsewhere,[14] that leads us to this conclusion. Whereas the resonant trapped electrons do not carry current, they nevertheless do absorb canonical toroidal angular momentum. In the absence of a mechanism for losing this momentum, such as collisions, they must drift toward the magnetic axis. (Collisions would simply distribute the current to circulating electrons, and, hence, are not relevant to the argument here.) In a true steady state, this inward drift must be balanced by an outward flux of electrons. An outward flux of electrons, however, drives the bootstrap current. Thus, the trapped electrons, while not directly carrying current, do generate an equivalent current through the bootstrap effect.

The crucial assumption here is that a steady state has been achieved. This may be safely assumed in reactors, but not in present-day tokamak experiments. For the bootstrap current to compensate for the current lost in the trapped electrons, the pressure produced by the inward drift must be high enough to force the compensating outward flow. This will occur only when $\beta_p \sim 1$, which is a higher β than that reached by most present-day tokamaks. On such tokamaks, experiments on low-frequency current drive will encounter complications due to trapped electrons, which will prefer to pinch inward rather than generate current.

We wish to remark that the calculations presented can apply even in situations where $\beta_p = 1$ is not achieved. The point is that mechanical angular momentum, injected into trapped electrons, increases the canonical angular momentum of the electrons even if no current is produced. The opportunity then exists for an efficient conversion of this momentum, which lies in the vector potential part of the canonical momentum, into electron mechanical momentum. The conversion may be achieved either by a pressure gradient, i.e., $\beta_p = 1$ as discussed here, or by some other means. Such other means could, for example, be the selective trapping and detrapping of electrons by cyclotron waves.[15] In principle, this conversion may be performed with negligible power dissipation. The calculation of J/P_d would then be governed by the primary process, i.e., momentum input via Alfvén waves, which is the calculation that we have presented.

Against our calculations that low-frequency current drive can be accomplished with less power dissipation than high-frequency current-drive must be set other reactor design criteria. Of paramount importance is the ability to place coils in a reactor environment. Until this problem is solved, the high-frequency method of current drive, which can utilize waveguides instead of coils, will remain more attractive even with higher power dissipation. We remark that recent considerations of the placement of limiters in reactor environments, e.g., Ref. 16, have relevance also to the placement of coils in that their design criteria are quite similar.

Finally, we wish to point out that although we have considered two highly favorable wave regimes in terms of power dissipation, we make no claim that there are not even more favorable regimes. In fact, as pointed out in Ref. 14, there exists the theoretical possibility of driving relatively collisionless electrons with waves with high-momentum content, thus exploiting the advantages of both wave regimes, while encountering neither disadvantage. This possibility, which relies on acceleration of electrons at the cyclotron resonance, does have drawbacks which may make it unfeasible. However, it does illustrate that the quest for the most efficient waves to drive currents in a tokamak reactor may not yet have uncovered the optimum wave.

ACKNOWLEDGMENTS

The authors appreciate discussions with F. W. Perkins and T. H. Stix.

This work was supported by the United States Department of Energy under Contract No. DE-AC02-CH03073.

[1] D. J. H. Wort, Plasma Phys. 13, 258 (1971).
[2] N. J. Fisch, Phys. Rev. Lett. 41, 873 (1978); 42, 410 (1979).
[3] C. F. F. Karney and N. J. Fisch, Phys. Fluids 22, 1817 (1979).
[4] J. M. Dawson and M. F. Uman, Nucl. Fusion 5, 242 (1965).
[5] T. H. Stix, Nucl. Fusion 15, 737 (1975).
[6] T. H. Dupree, Phys. Fluids 9, 1773 (1966).
[7] M. N. Rosenbluth, W. M. MacDonald, and D. L. Judd, Phys. Rev. 107, 1 (1957).
[8] B. A. Trubnikov, in *Reviews of Plasma Physics*, edited by M. A. Leontovich (Consultants Bureau, New York, 1967), Vol. 3, p. 229.
[9] J. S. Chang and G. Cooper, J. Comput. Phys. 6, 1 (1970).
[10] A. Hasegawa and L. Chen, Phys. Fluids 19, 1924 (1976).
[11] C. F. F. Karney, F. W. Perkins, and Y.-C. Sun, Phys. Rev. Lett. 42, 1621 (1979).
[12] D. A. Ehst, Nucl. Fusion 19, 1369 (1979).
[13] R. J. Bickerton, Comments Plasma Phys. Controlled Fusion 1, 95 (1972).
[14] N. J. Fisch, in *Proceedings of the Second Joint Varenna-Grenoble International Symposium on Heating in Toroidal Plasma*, Como, Italy, 1980 (Pergamon Press, New York, 1980, to be published).
[15] T. Ohkawa, General Atomic Report GA-A13847 (1976).
[16] R. W. Conn, I. N. Sviatoslavsky, and D. K. Sze, presented at the IEEE Meeting on Engineering Problems of Fusion Research (1979).